

ORIGINAL ARTICLE

Open Access



Development and validation of a model for predicting the expression of Ki-67 in pancreatic ductal adenocarcinoma with radiological features and dual-energy computed tomography quantitative parameters

Youjia Wen¹, Zuhua Song¹, Qian Li¹, Dan Zhang¹, Xiaojiao Li¹, Jiayi Yu¹, Zongwen Li¹, Xiaofang Ren¹, Jiayan Zhang¹, Qian Liu¹, Jie Huang¹, Dan Zeng¹ and Zhuoyue Tang^{1*}

Abstract

Objective To construct and validate a model based on the dual-energy computed tomography (DECT) quantitative parameters and radiological features to predict Ki-67 expression levels in pancreatic ductal adenocarcinoma (PDAC).

Materials and methods Data from 143 PDAC patients were analysed. The variables of clinic, radiology and DECT were evaluated. In the arterial phase and portal venous phase (PVP), the normalized iodine concentration (NIC), normalized effective atomic number and slope of the spectral attenuation curves were measured. The extracellular volume fraction (ECVf) was measured in the equilibrium phase. Univariate analysis was used to screen independent risk factors to predict Ki-67 expression. The Radiology, DECT and DECT–Radiology models were constructed, and their diagnostic effectiveness and clinical applicability were obtained through area under the curve (AUC) and decision curve analysis, respectively. The nomogram was established based on the optimal model, and its goodness-of-fit was assessed by a calibration curve.

Results Computed tomography reported regional lymph node status, NIC of PVP, and ECVf were independent predictors for Ki-67 expression prediction. The AUCs of the Radiology, DECT, and DECT–Radiology models were 0.705, 0.884, and 0.905, respectively, in the training cohort, and 0.669, 0.835, and 0.865, respectively, in the validation cohort. The DECT–Radiology nomogram was established based on the DECT–Radiology model, which showed the highest net benefit and satisfactory consistency.

Conclusions The DECT–Radiology model shows favourable predictive efficacy for Ki-67 expression, which may be of value for clinical decision-making in PDAC patients.

*Correspondence:

Zhuoyue Tang

zhuoyue_tang@cqmu.edu.cn

Full list of author information is available at the end of the article

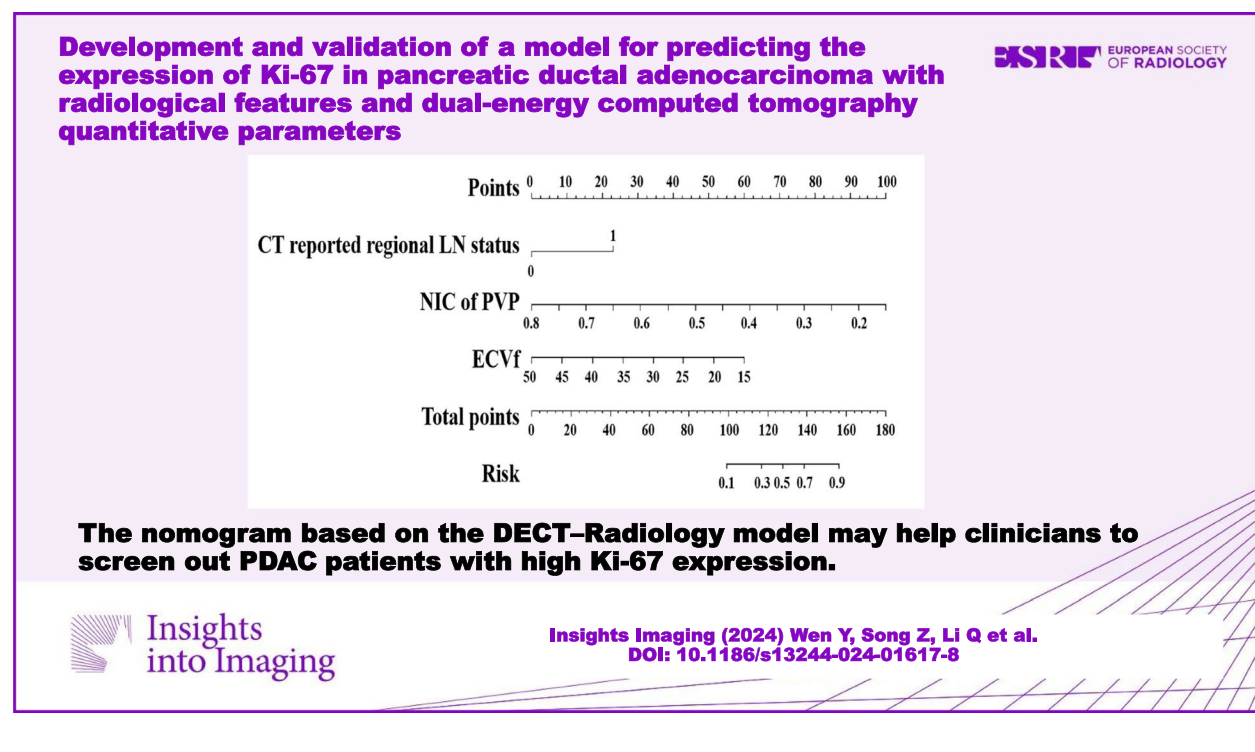
Critical relevance statement The DECT–Radiology model could contribute to the preoperative and non-invasive assessment of Ki-67 expression of PDAC, which may help clinicians to screen out PDAC patients with high Ki-67 expression.

Key points

- Dual-energy computed tomography (DECT) can predict Ki-67 in pancreatic ductal adenocarcinoma (PDAC).
- The DECT–Radiology model facilitates preoperative and non-invasive assessment of PDAC Ki-67 expression.
- The nomogram may help screen out PDAC patients with high Ki-67 expression.

Keywords Dual-energy computed tomography (DECT), Pancreatic ductal adenocarcinoma (PDAC), Ki-67, Prognosis, Nomogram

Graphical Abstract



Introduction

Pancreatic ductal adenocarcinoma (PDAC), an extremely malignant and invasive tumour, is estimated to be the second principal cause of cancer-related death globally in 2030 [1]. PDAC progresses rapidly, and most patients already have lymph nodes or distant metastases when the time of diagnosis is confirmed [2, 3]. Although advances in multimodal therapy have improved, the 5-year survival rate for PDAC has not increased obviously and remains at approximately 11% [4–6]. Ki-67 possesses high expression in the majority of proliferating cells except for G0, which is one of the important immunohistochemical markers designating tumour heterogeneity and cell growth and can

accurately reflect the proliferative activity of tumour cells [7]. Previous inquiries have suggested a negative relationship between the expression level of Ki-67 and the differentiation degree of PDAC tumours, and PDAC patients with high Ki-67 expression levels were more likely to develop metastases in regional lymph nodes (LNs) and the liver [8–10]. Ki-67 was also an independent risk factor for the poor prognosis of PDAC and the recurrence within 1 year after pancreaticoduodenectomy [8, 10]. Therefore, accurately evaluating the degree of Ki-67 expression is important for judging the prognosis of PDAC.

Currently, the expression of Ki-67 can only be determined by immunohistochemistry (IHC) on puncture or

surgical specimens. Nevertheless, a single puncture may not always be successful in sampling, and the resulting multiple punctures may cause multiple injuries and inconveniences to the patient [11]. Furthermore, biopsy and surgical specimens are invasive methods that may induce tumour ulcers or breaches to increase the risk of tumour spread. Hence, it is crucial to create a noninvasive, convenient and effective measure to predict the level of Ki-67 expression in PDAC.

Dual-energy computed tomography (DECT) uses two X-ray sources with different energy levels to image objects and has shown prospects for clinical applications in the detection and characterization of tumours. Various quantitative metrics derived from DECT, such as normalized iodine concentration (NIC), normalized effective atomic number (N_{Ze}) and slope of the spectral HU curve (λ HU), have been gradually applied to predict the Ki-67 in various types of solid tumours, including laryngeal squamous cell carcinoma, breast cancer, and gastric adenocarcinoma [12–14]. As an emerging quantitative DECT parameter, extracellular volume fraction (ECVf) has also been applied to evaluate the efficacy of radiotherapy and survival analysis with neoadjuvant chemotherapy in PDAC [15, 16]. However, the association between DECT-derived parameters and the degree of Ki-67 expression in PDAC patients is ill-defined and infrequently reported. Meanwhile, preoperative radiological features such as the presence of focal pancreatic parenchymal atrophy, pancreatic duct expansion, peritumoural vessel invasion and extrapancreatic perineural invasion were found to indicate the poor prognosis of PDAC patients [17–20], and have an important impact on the treatment decision of PDAC.

In this research, we supposed that DECT quantitative parameters could predict Ki-67 expression in PDAC. To prove our assumption, we attempt to establish a model binding DECT quantitative parameters and radiological features to recognize patients with high Ki-67 expression and visualize it as a nomogram for assisting in the realization of individualized clinical decision-making in PDAC patients.

Materials and methods

Patients

The research obtained consent from the Ethics Committee of the Chongqing General Hospital. Owing to the retrospective nature of the study, we waived the requirement for informed consent from the participants. Data on patients with pathologically confirmed PDAC and examined Ki-67 were continuously collected at Chongqing General Hospital from July 2021 to April 2023 based on inclusion and exclusion criteria (Fig. 1). The inclusion criteria were as follows: (1) PDAC was confirmed by biopsy or surgery; (2) Ki-67 was examined by IHC; and

(3) DECT was performed within 14 days of the examination of Ki-67. The exclusion criteria were as follows: (1) neoadjuvant chemotherapy or radiotherapy before Ki-67 examination; (2) unsatisfactory image quality for analysis; (3) merged other primary malignancies; and (4) partially missing clinical, pathological, surgical or imaging data.

Eventually, 143 patients (81 men and 62 women; mean age \pm SD, mean age 62.57 ± 0.86 years) were recruited and were further randomly divided into the training and validation cohorts at a ratio of 7:3 ($n = 100, 70.0\%$; 43, 30.0%).

Ki-67 index measurement

The Ki-67 of the 143 patients was examined by IHC performed on surgical specimens (52.4%) and percutaneous or transgastric core biopsy specimens (47.6%). All specimens were from primary pancreatic tumours. Cells with brown nuclei were defined as positive. The Ki-67 was 0–100% based on the proportion of 1000 positive cells randomly selected at 200 \times magnification. Since the optimal cut-off value for the Ki-67 low or high differentiation set of PDAC has not been determined, 50% was chosen as the cut-off on the basis of previous studies [8]. The samples were divided into a low Ki-67 expression set (Ki-67 $\leq 50\%$) and a high Ki-67 expression set (Ki-67 $> 50\%$).

DECT image acquisition

Contrast-enhanced abdominal scans were performed using a DECT (IQon spectral CT, Philips Healthcare). All DECT scans were performed by scanners using a standard protocol, with details described in the [Supplementary material](#).

Radiology and DECT candidate variables

The radiological candidate variables of PDAC included tumour location, CT-reported T stage, CT-reported regional LN status, atrophy of the pancreatic parenchyma, expansion of the main pancreatic duct, blood vessels invasion and extrapancreatic perineural invasion. The DECT candidate variables of PDAC included NIC, N_{Ze} and λ HU in the arterial phase (AP) and portal vein phase (PVP), and the extracellular volume fraction (ECVf) in the equilibrium phase (EP). Details are described in the [Supplementary material](#).

Construction of the models and nomogram

The differences in variables between low and high Ki-67 expression sets were contrasted with univariate analysis first. The independent risk factors for predicting the Ki-67 expression of PDAC patients were ascertained after forward stepwise binary logistic regression from the significant parameters ($p < 0.05$) in the training cohort. Next, the Radiology, DECT and DECT–Radiology models were built depending on the independent hazard

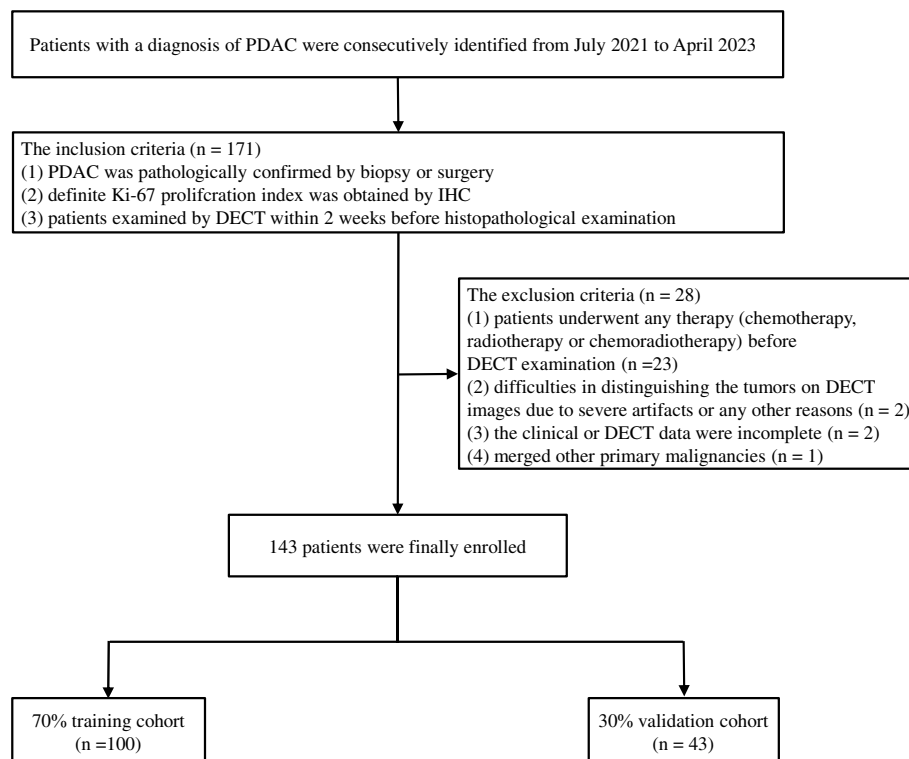


Fig. 1 Flowchart of the participant inclusion process. PDAC, pancreatic ductal adenocarcinoma; IHC, immunohistochemistry; DECT, dual-energy computed tomography

elements. The above models were independently proven in the validation cohort. The diagnostic effectiveness and clinical applicability of the three models were obtained through receiver operating characteristic curve (ROC) and decision curve analysis (DCA). The contrast for the area under the curve (AUC) was determined through the Delong test. Finally, a nomogram was developed from the model with the highest diagnostic performance. The goodness-of-fit of the nomogram was evaluated through the calibration curve.

Statistical analysis

All calculations and statistical analyses were executed in R software (<https://www.r-project.org/>), MedCalc (version 18.2.1, MedCalc Software) and SPSS software (version 26.0, SPSS, IBM). The Shapiro–Wilk test was utilized to verify the data normality. The data were demonstrated as the mean \pm standard deviation (SD) for normally distributed data and as the median (25th, 75th percentiles) for non-normally distributed data. Continuous variables were estimated through a two-sample *t* test or Mann–Whitney *U* test. Categorical variables were estimated through the chi-square test. A two-sided *p* value < 0.05 declared statistical significance.

Results

Radiological features and DECT quantitative parameters

Table 1 displays variables from the clinic, radiology and DECT of the study. In the training cohort, the CT-reported regional LN status and all DECT quantitative parameters demonstrated significant differences with $p < 0.05$. Table 2 displays the representation of DECT quantitative parameters in the training cohort, including the mean values of λ HU of PVP and the median values of NIC of AP, λ HU of AP and NZeff of AP, NIC of PVP, NZeff of PVP and the ECVf. The above DECT quantitative parameters of the low Ki-67 expression set were significantly higher than those of the high Ki-67 expression set ($p < 0.05$). Statistically significant differences were not found in any clinical characteristics, tumour location, CT-reported T stage, parenchyma atrophy, pancreatic duct expansion or vessels invasion between the low Ki-67 expression set and the high Ki-67 expression set ($p > 0.05$).

Development of prediction models for Ki-67 expression

Multivariate logistic regression analysis was used to analyse all variables with $p < 0.05$ (Table 3). The CT-reported regional LN status (OR = 5.787; 95% CI: 1.392–24.066; $p = 0.016$), NIC of PVP (OR = 0.170; 95% CI: 0.044–0.656;

Table 1 Variables of clinic, radiology and DECT in the training and validation cohorts

Variables	Training cohort (n = 100)	Validation cohort (n = 43)
Clinical characteristics		
Gender (%)		
Male	56 (56.0)	25 (58.1)
Female	44 (44.0)	18 (41.9)
Age (mean \pm SD)	62.60 \pm 10.55	62.49 \pm 9.74
BMI (mean \pm SD)	22.31 \pm 2.76	21.57 \pm 3.33
CEA (%)		
Normal	69 (69.0)	36 (83.7)
Elevated	31 (31.0)	7 (16.3)
CA-125 (%)		
Normal	61 (61.0)	30 (69.8)
Elevated	39 (39.0)	13 (30.2)
CA-199 (%)		
Normal	20 (20.0)	7 (16.3)
Elevated	80 (80.0)	36 (83.7)
Radiological features		
Tumour location (%)		
Head and neck	70 (70.0)	27 (62.8)
Body and tail	30 (30.0)	16 (37.2)
CT-reported T stage (%)		
T1–T2	54 (54.0)	23 (53.5)
T3–T4	46 (46.0)	20 (46.5)
CT-reported regional LN status (%)		
Negative	49 (49.0)	19 (44.2)
Positive	51 (51.0)	24 (55.8)
Parenchyma atrophy (%)		
Negative	63 (63.0)	20 (46.5)
Positive	37 (37.0)	23 (53.5)
Pancreatic duct expansion (%)		
Negative	32 (32.0)	17 (39.5)
Positive	68 (68.0)	26 (60.5)
Vessels invasion (%)		
Negative	72 (72.0)	32 (74.4)
Positive	28 (28.0)	11 (25.6)
Extrapancreatic perineural invasion status (%)		
Negative	33 (33.0)	12 (27.9)
Positive	67 (67.0)	31 (72.1)
DECT quantitative parameters		
NIC of AP	0.09 \pm 0.04	0.08 \pm 0.03
NZeff of AP	0.68 \pm 0.04	0.68 \pm 0.05
λ HU of AP	1.37 \pm 0.52	1.22 \pm 0.50
NIC of PVP	0.38 \pm 0.11	0.37 \pm 0.07
NZeff of PVP	0.87 \pm 0.05	0.86 \pm 0.03
λ HU of PVP	2.30 \pm 0.70	2.09 \pm 0.54
ECVf (%*)	36.08 \pm 6.52	35.18 \pm 6.69

The % value reflects the composition ratio

The %* value reflects the percentages

AP arterial phase, DECT dual-energy computed tomography, ECVf the extracellular volume fraction, LN lymph node, NIC normalized iodine concentration, NZeff normalized effective atomic number, PVP portal venous phase, SD standard deviation, λ HU slope of the spectral Hounsfield unit curve

Table 2 Univariate analysis for the variables of clinic, radiology and DECT for differentiating between low and high Ki-67 expression sets in the training cohort

Variables	Low Ki-67 expression set (Ki-67 \leq 50%, $n = 77$)	High Ki-67 expression set (Ki-67 $>$ 50%, $n = 23$)	F/Z/ χ^2	p value
BMI	22.40 \pm 2.84	22.00 \pm 2.50	2.112	0.538
CEA (%)			0.337	0.562
Normal	52 (67.5)	17 (73.9)		
Elevated	25 (32.5)	6 (26.1)		
CA-125 (%)			0.978	0.323
Normal	49 (63.6)	12 (52.2)		
Elevated	28 (36.4)	11 (47.8)		
CA-199 (%)			3.391	0.066
Normal	19 (24.7)	1 (4.3)		
Elevated	58 (75.3)	22 (95.7)		
Tumour location (%)			0.325	0.568
Head and neck	55 (71.4)	15 (65.2)		
Body and tail	22 (28.6)	8 (34.8)		
CT-reported T stage (%)			0.076	0.782
T1–T2	41 (53.2)	13 (56.5)		
T3–T4	36 (46.8)	10 (43.5)		
CT-reported regional LN status (%)			10.36	< 0.001
Negative	45 (58.4)	4 (17.4)		
Positive	32 (41.6)	19 (82.6)		
Parenchyma atrophy (%)			1.502	0.220
Negative	51 (66.2)	12 (52.2)		
Positive	26 (33.8)	11 (47.8)		
Pancreatic duct expansion (%)			0.034	0.854
Negative	25 (32.5)	7 (30.4)		
Positive	52 (67.5)	16 (69.6)		
Vessels invasion (%)			0.088	0.766
Negative	56 (72.7)	16 (69.6)		
Positive	21 (27.3)	7 (30.4)		
Extrapaneatic perineural invasion status (%)			0.008	0.928
Negative	51 (66.2)	15 (65.2)		
Positive	26 (33.8)	8 (34.8)		
NIC of AP	0.09 (0.07, 0.12)	0.06 (0.04, 0.08)	− 3.051	0.002
NZeff of AP	0.66 (0.64, 0.67)	0.64 (0.61, 0.65)	− 1.994	0.046
λ HU of AP	1.09 (0.78, 1.42)	0.77 (0.58, 1.03)	− 3.94	< 0.001
NIC of PVP	0.33 (0.30, 0.39)	0.24 (0.22, 0.29)	− 4.902	< 0.001
NZeff of PVP	0.86 (0.84, 0.87)	0.83 (0.80, 0.84)	− 4.149	< 0.001
λ HU of PVP	2.48 \pm 0.66	1.69 \pm 0.44	3.354	< 0.001
ECVf (%)	34.70 (31.72, 37.87)	26.15 (20.97, 31.02)	− 5.197	< 0.001

The % value reflects the composition ratio

The %* value reflects the percentages

F/Z/ χ^2 values represent the statistics of two independent sample *t*-tests for normal distribution, two independent sample *t*-tests for non-normal distribution and chi-square test, respectively

AP arterial phase, DECT dual-energy computed tomography, ECVf the extracellular volume fraction, LN lymph node, NIC normalized iodine concentration, NZeff normalized effective atomic number, PVP portal venous phase, λ HU slope of the spectral Hounsfield unit curve

Table 3 Forward stepwise logistic regression analysis for the significant variables of radiology and DECT as predicting the expression of Ki-67 of PDAC in the training cohort

Variables	Odds ratio	95% CI	p value
CT-reported regional LN status	5.787	1.392–24.066	0.016
NIC of PVP	0.170	0.044–0.656	0.010
ECVf (%)	0.879	0.782–0.988	0.030

DECT dual-energy computed tomography, ECVf the extracellular volume fraction, LN lymph node, NIC normalized iodine concentration, PVP portal venous phase

$p=0.010$) and ECVf (OR=0.879; 95% CI: 0.782–0.988; $p=0.030$) were screened out through forward stepwise logistic regression. The Radiology, DECT and DECT–Radiology models were then established on the basis of the independent risk factors. The Radiology, DECT and

DECT–Radiology models were severally proved independently in the validation cohort.

Diagnostic performances of the three models

Predictive outcomes of the three models are shown in Table 4. Figures 2 and 3 display the ROC and DCA to identify low and high Ki-67 expression in the two cohorts for the three models. The Radiology model produced moderate diagnostic performances of Ki-67 expression in PDAC patients in the training and validation cohorts, with AUCs of 0.705 (95% CI: 0.590–0.820) and 0.669 (95% CI: 0.499–0.839), respectively. Both the DECT model and the DECT–Radiology model produced preferable diagnostic performances in distinguishing the Ki-67 proportion in PDAC patients, with AUCs of 0.884 (95% CI: 0.816–0.952) and 0.905 (95% CI: 0.826–0.883) in the training cohort. Correspondingly, the DECT model and DECT–Radiology

Table 4 Diagnostic performance of the Radiology, DECT and DECT–Radiology models in the training and validation cohorts

Models	Training cohort				Validation cohort			
	AUC (95% CI)	SEN	SPE	DeLong	AUC (95% CI)	SEN	SPE	DeLong
Radiology model	0.705 (0.590–0.820)	0.826	0.587	0.001 ^a	0.669 (0.499–0.839)	0.786	0.552	0.093 ^a
DECT model	0.884 (0.816–0.952)	0.913	0.779	0.300 ^b	0.835 (0.715–0.955)	0.786	0.828	0.514 ^b
DECT–Radiology model	0.905 (0.841–0.968)	0.826	0.883	<0.001 ^c	0.865 (0.757–0.972)	0.857	0.793	0.003 ^c

AUC area under the curve, CI confidence interval, DECT dual-energy computed tomography, SEN sensitivity, SPE specificity

^a Radiology model versus DECT model

^b DECT model versus DECT–Radiology model

^c DECT–Radiology versus Radiology model

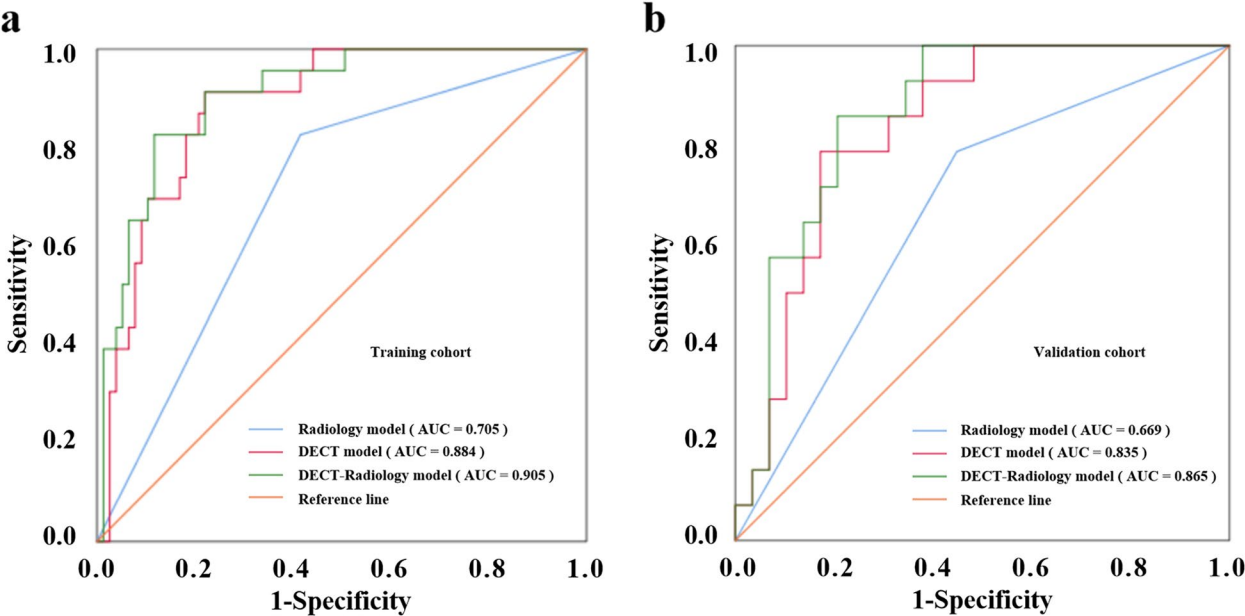


Fig. 2 ROCs of Radiology model, DECT model, and DECT–Radiology model for predicting the expression of Ki-67 of PDAC in the training and validation cohorts (a, b). AUC, area under the curve; ROC, receiver operating characteristic curve; DECT, dual-energy computed tomography

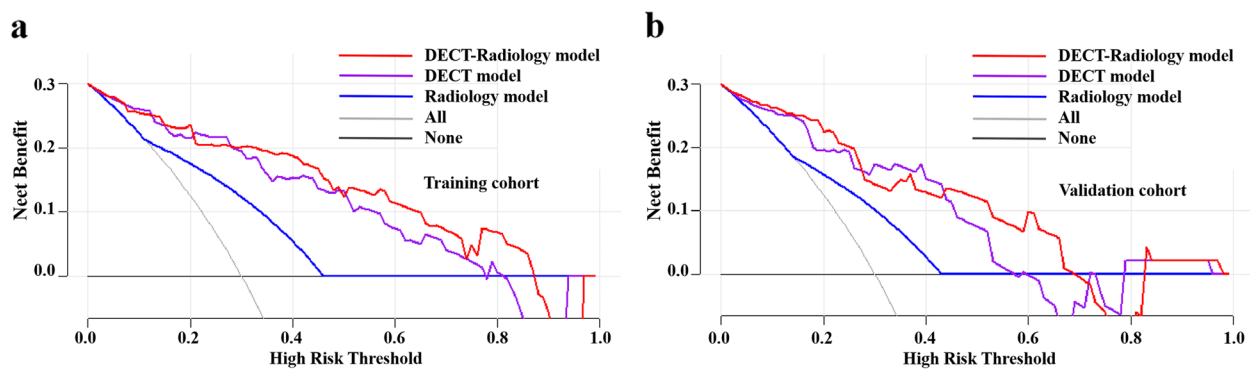


Fig. 3 DCA outcomes for the models of Radiology, DECT, and DECT–Radiology. The y-axis and x-axis demonstrate the net benefit and threshold probability respectively. The black line represents all cases that are assumed to be high Ki-67 expression, and the grey line represents all cases that are assumed to be low Ki-67 expression. The DCA demonstrated that DECT–Radiology model was more advantageous than the Radiology model and DECT model (**a, b**). DCA, decision curve analysis; DECT, dual-energy computed tomography

model had AUCs of 0.835 (95% CI: 0.715–0.955) and 0.865 (95% CI: 0.757–0.972), respectively, in the validation cohort. The DeLong test revealed that the DECT–Radiology model performed better than the Radiology model in the training ($p < 0.001$). The diagnostic presentation of the DECT model improved compared with that of the Radiology model ($p = 0.001$) in the training cohort, however, there were non-existent statistically significant differences in the validation cohort ($p = 0.093$). DCA findings revealed that the DECT–Radiology model could produce a higher net benefit for the ranges of the 0.04–0.90 and 0.04–0.70 threshold probabilities in the training and validation cohorts, respectively.

Development and performance of DECT–radiology nomogram

The DECT–Radiology nomogram was established based on the DECT–Radiology model that possessed the highest diagnostic efficacy for anticipating the expression of

Ki-67 in PDAC (Fig. 4). The parameters of the DECT–Radiology nomogram including the CT-reported regional LN status, NIC of PVP and ECVf. The formula was as follows: DECT–Radiology nomogram = $1.787 \times \text{CT-reported regional LN status} - 11.921 \times \text{NIC of PVP} - 0.133 \times \text{ECVf} + 6.294$. A good consistency between the predicted and actual probabilities of the nomogram was observed in the calibration curve analysis in predicting the level of Ki-67 in PDAC in the training and validation cohorts (Fig. 5).

Representative images are shown in Fig. 6.

Discussion

In this retrospective study, a DECT–Radiology model consisting of CT-reported regional LN status, NIC of PVP, and ECVf was developed and validated to achieve the noninvasive prediction of the degree of Ki-67 expression in PDAC. The level of Ki-67 expression was positively correlated with PDAC tumour grade and ultimately disease stage [21]. For high-stage

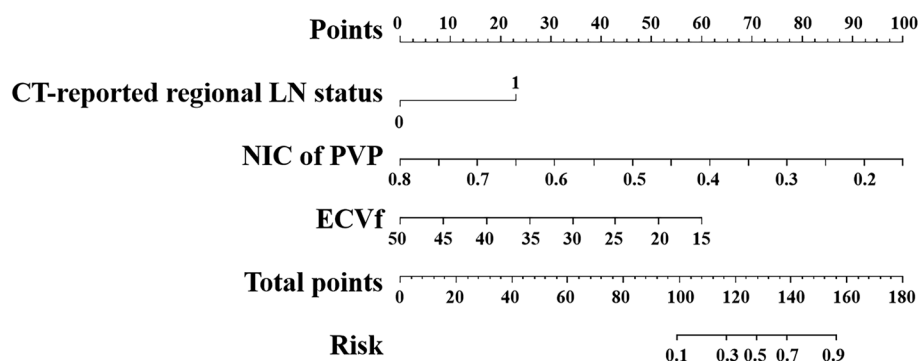


Fig. 4 DECT–Radiology nomogram was diagramed uniting one radiological and two DECT variables. The points of each predictive index are scored by the corresponding values on “point line”. The total scores are obtained from the summation of the points of all predictive indexes to assess the Ki-67 expression in PDAC. CT, computed tomography; DECT, dual-energy computed tomography; ECVf, the extracellular volume fraction; LN, lymph node; NIC, normalized iodine concentration; PDAC, pancreatic ductal adenocarcinoma; PVP, portal venous phase

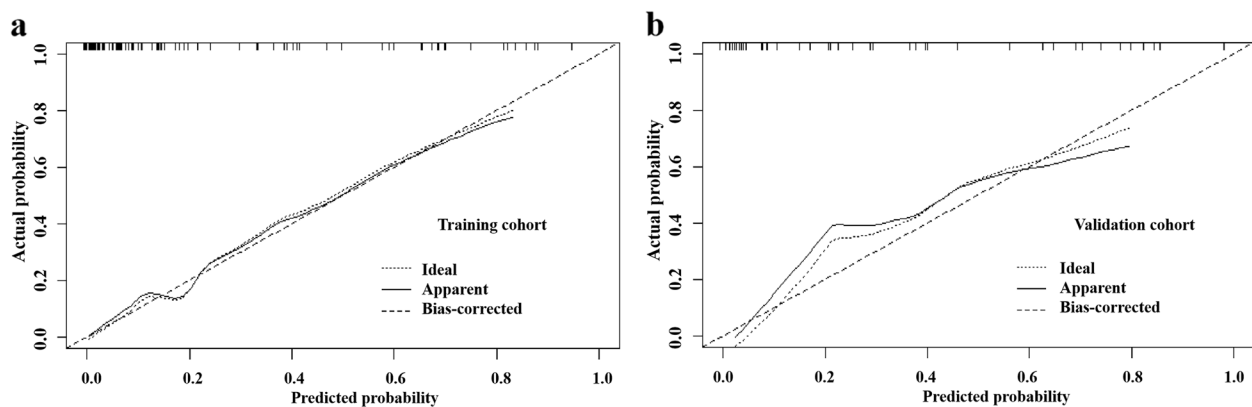


Fig. 5 Calibration curves of DECT-Radiology nomogram in cohorts of training and validation (**a**, **b**). Diagonal implies DECT-Radiology nomogram of an ideal performance. Closer to the diagonal implies more accuracy. DECT, dual-energy computed tomography

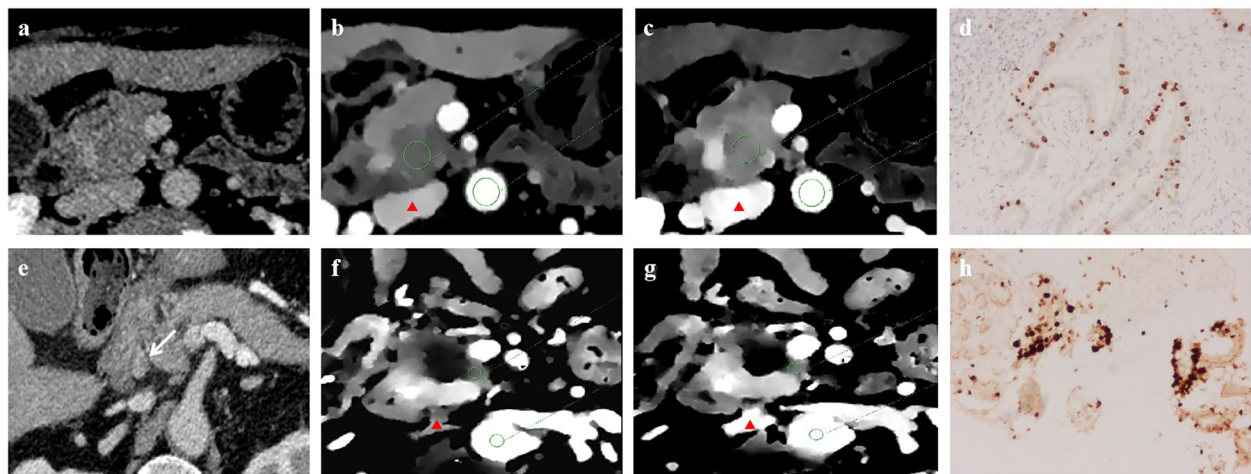


Fig. 6 DECT figures of a 66-year-old female patient with low Ki-67 expression in PDAC. **a** CT-reported regional LN negative. **b**, **c** IC_{tumour} and IC_{aorta} in the same layer in the PVP and EP, the NIC of PVP was 0.45 mg/ml and the ECVf was 42.29%. **d** Ki-67 was 30%. (red arrow: inferior vena cava). DECT figures of a 73-year-old male patient with high Ki-67 expression in PDAC. **e** CT-reported regional LN positive. **f**, **g** IC_{tumour} and IC_{aorta} in the same layer in the PVP and EP, the NIC of PVP was 0.34 mg/ml and the ECVf was 37.08%. **h** Ki-67 expression was 60%. (red arrow: inferior vena cava). DECT, dual-energy computed tomography; ECVf, extracellular volume fraction; EP, equilibrium phase; IC, iodine concentration; LN, lymph node; NIC, normalized iodine concentration; PDAC, pancreatic ductal adenocarcinoma; PVP, portal vein phase

PDAC patients, neoadjuvant therapy (NAC) can prolong disease-specific survival and disease-free survival [22]. Therefore, PDAC patients with high levels of Ki-67 expression may benefit from receiving aggressive NAC. The nomogram derived from the DECT-Radiology model demonstrated better identification ability than the Radiology and DECT models in both the training and validation cohorts in predicting Ki-67 expression, which may be an effective imaging tool to preoperatively and noninvasively identify PDAC patients with high levels of Ki-67 expression.

We discovered that the CT-reported regional LN status was the most important radiological feature to

distinguish the degree of Ki-67 expression in PDAC. A higher positive rate of CT-reported regional LN status was found in the high Ki-67 expression set than in the low Ki-67 expression set (82.6% vs 41.5%). The Radiology model was constructed based on this independent indicator and achieved moderate diagnostic effectiveness, with AUCs reaching 0.705 and 0.669 in the training and validation cohorts, respectively. Departed studies have pointed out that PDAC patients with higher levels of Ki-67 expression were more prone to regional LN metastasis [10]. It has been shown that CT-reported LN status significantly correlates with

pathological status [23]. The reason that CT-reported regional LN status could predict Ki-67 expression may be because Ki-67 reflects the degree of tumour proliferation activity, and a higher degree of expression indicates that the tumour has more active tumour proliferation and is more likely to infiltrate through the wall of lymphatic vessels and develop lymph node metastasis. However, the judgement of LN metastasis in CT was mainly based on the enhanced and margin status and other indicators, which had certain subjective dependence. Previous studies have discovered the low accuracy of CT for assessing peripancreatic LNM (63%–81%), which was similarly confirmed in our study (66.7%) [24, 25]. Although some radiological features such as parenchyma atrophy and extrapancreatic perineural invasion status have been documented as significant prognostic indicators of PDAC, there were no statistical differences between high and low Ki-67 expression sets and still inability to be used as predictors of Ki-67 expression. This indicated that it was insufficient to assess the Ki-67 expression level by relying on morphological characteristics alone, and blood supply characteristics or internal characteristics may provide comprehensive information.

In this study, our results also indicated that the NIC of PVP and ECVf were independent risk factors for predicting the expression of Ki-67 in PDAC in the series of DECT quantitative parameters. The parameter NIC was obtained through normalized IC, which minimized inter-individual hemodynamic variations, and could quantitatively show the extent of tumour neovascularization and objectively reflect iodine deposition in tissues [26]. In our study, the NIC of PVP in the Ki-67 high expression set was significantly lower than that in the Ki-67 low expression set in the training cohort (0.33 vs. 0.24, $p < 0.001$). The possible reasons for this were the fact that high Ki-67 expression represents active cell proliferation, whereas ischaemia and hypoxia due to active cell proliferation in PDAC constitute the microenvironment for the growth of PDAC and that PDAC is a less vascular tumour with a high fibrous stromal component [27]. The ECVf is a quantitative indicator of the extravascular space and extracellular space, and the extravascular space and extracellular space are important parts of the cellular microenvironment. The evolution of tumours is accompanied by changes in the extracellular microenvironment, so the extracellular matrix can partly reflect the development of disease. In our study, the ECVf was significantly lower than that in the low Ki-67 expression set (26.15% vs 34.80%, $p < 0.001$). A previous study revealed that low ECVf indicated poor vascularization for those more prone to hypoxia, which may explain why ECVf could predict the expression status of Ki-67 [15]. The

DECT model built on the basis of the NIC of PVP and ECVf had a better diagnostic ability than the Radiology model, in which the AUCs were 0.884 and 0.835 for the training and validation cohorts, respectively.

By incorporating the CT-reported regional LN status, NIC of PVP and ECVf, we established the DECT–Radiology model that emerged with the highest diagnostic efficacy (training cohort: 0.905; validation cohort: 0.865) and net benefits through comparison with the Radiology model and the DECT model. This DECT–Radiology model showed significantly better diagnostic efficacy for the expression of Ki-67 in patients with PDAC than the Radiology model in the training and validation cohorts (all $p < 0.05$, DeLong test). The DECT–Radiology nomogram, a simple, potentially reliable and reproducible tool, was established on the basis of the DECT–Radiology model and possessed the highest diagnostic ability for predicting Ki-67 expression in PDAC. Good agreement between prediction and observation was demonstrated in the calibration curve in both the training cohort and validation cohort.

This study had some limitations. First, this study was retrospective, and the selection of samples may still exist in a biased manner despite strict inclusion and exclusion criteria. Second, because the sample scale of this study was small and conducted in one infirmary, further multicentre large-scale studies are needed to verify the findings before the DECT–Radiology nomogram can be applied in clinical practice. Finally, some of the samples in this study were puncture biopsies, which were not fully representative of all tumour tissues due to tumour heterogeneity and may lead to some bias in Ki-67 measurements. Most PDAC patients were unable to undergo radical resection to obtain a surgical specimen at the advanced stage at the time of initial medical consultation, whereas puncture biopsy could assist in individualized clinical decision-making.

Conclusion

In conclusion, a model that combines key radiological features and dual-energy computed tomography quantitative parameters is helpful in the preoperative and non-invasive evaluation of the Ki-67 expression in patients with PDAC. The visualized nomogram constructed based on the DECT–Radiology model is simple and effective and may help clinicians to screen out PDAC patients with high Ki-67 expression.

Abbreviations

AP	Arterial phase
AUC	Area under the curve
CI	Confidence interval
DCA	Decision curve analysis
DECT	Dual-energy computed tomography
ECVf	Extracellular volume fraction

EP	Equilibrium phase
IHC	Immunohistochemistry
LN	Lymph node
NAC	Neoadjuvant therapy
NIC	Normalized iodine concentration
NZeff	Normalized effective atomic number
PDAC	Pancreatic ductal adenocarcinoma
PVP	Portal venous phase
ROC	Receiver operating characteristic curve
SD	Standard deviation
λHU	Slope of the spectral attenuation curves

Supplementary Information

The online version contains supplementary material available at <https://doi.org/10.1186/s13244-024-01617-8>.

Additional file 1.

Authors' contributions

YJW, ZHS and ZYT proposed the design of the study. QL, DZ, XJL, JYY, ZWL, XFR, JYZ, QL and JH collected the data. YJW and ZHS analysed the data. YJW wrote the first draft. All authors read and approved the final manuscript.

Funding

This work was supported by the Medical Research Joint Key Project of Chongqing Health Commission and Science and Technology Bureau in China (Grant: 2019ZDXM010); the Medical Scientific Research Joint Project of Chongqing Health Commission and Science and Technology Bureau in China (Grant: 2020FYX151).

Availability of data and materials

The data underlying this article cannot be shared publicly for the privacy of individuals who participated in the study. The data will be provided by the corresponding author on sensible request.

Declarations

Ethics approval and consent to participate

This study was permitted by the Institutional Review Board of Chongqing General Hospital, and the requirement of informed consent from the study participants was waived due to the retrospective nature of this study.

Consent for publication

Not applicable.

Competing interests

The authors declare that they have no competing interests.

Author details

¹Chongqing General Hospital, No.118, Xingguang Avenue, Liangjiang New Area, Chongqing, China.

Received: 12 September 2023 Accepted: 21 December 2023

Published online: 14 February 2024

References

- Rahib L, Smith BD, Aizenberg R, Rosenzweig AB, Fleshman JM, Matrisian LM (2014) Projecting cancer incidence and deaths to 2030: the unexpected burden of thyroid, liver, and pancreas cancers in the United States. *Cancer Res* 74:2913–2921. <https://doi.org/10.1158/0008-5472.CAN-14-0155>
- Bian Y, Zheng Z, Fang X et al (2023) Artificial intelligence to predict lymph node metastasis at CT in pancreatic ductal adenocarcinoma. *Radiology* 306:160–169. <https://doi.org/10.1148/radiol.220329>
- Akatori T, Shio M, Yanagimoto H et al (2019) Phase II study of the triple combination chemotherapy of SOXIRI (S-1/Oxaliplatin/Irinotecan) in patients with unresectable pancreatic ductal adenocarcinoma. *Oncologist* 24:749–e224. <https://doi.org/10.1634/theoncologist.2018-0900>
- Sung H, Ferlay J, Siegel RL et al (2021) Global cancer statistics 2020: GLOBOCAN estimates of incidence and mortality worldwide for 36 cancers in 185 countries. *CA Cancer J Clin* 71:209–249. <https://doi.org/10.3322/caac.21660>
- Sántha P, Lenggenhager D, Finstadsveen A et al (2021) Morphological heterogeneity in pancreatic cancer reflects structural and functional divergence. *Cancers (Basel)* 13:895. <https://doi.org/10.3390/cancers13040895>
- Haeblerle L, Insilla AC, Kapp AC et al (2021) Stroma composition and proliferative activity are related to therapy response in neoadjuvant treated pancreatic ductal adenocarcinoma. *Histol Histopathol* 36:733–742. <https://doi.org/10.14670/HH-18-332>
- Zheng YM, Chen J, Zhang M et al (2023) CT radiomics nomogram for prediction of the Ki-67 index in head and neck squamous cell carcinoma. *Eur Radiol* 33:2160–2170. <https://doi.org/10.1007/s00330-022-09168-6>
- Pergolini I, Crippa S, Pagnanelli M et al (2019) Prognostic impact of Ki-67 proliferative index in resectable pancreatic ductal adenocarcinoma. *BJS Open* 3:646–655. <https://doi.org/10.1002/bjs5.50175>
- Kawahara K, Takano S, Furukawa K, Takayashiki T, Kuboki S, Ohtsuka M (2022) The effect of the low stromal ratio induced by neoadjuvant chemotherapy on recurrence patterns in borderline resectable pancreatic ductal adenocarcinoma. *Clin Exp Metastasis* 39:311–322. <https://doi.org/10.1007/s10585-021-10142-7>
- Kim H, Park CY, Lee JH, Kim JC, Cho CK, Kim HJ (2015) Ki-67 and p53 expression as a predictive marker for early postoperative recurrence in pancreatic head cancer. *Ann Surg Treat Res* 88:200–207. <https://doi.org/10.4174/ast.2015.88.4.200>
- Acs B, Leung SCY, Kidwell KM et al (2022) Systematically higher Ki67 scores on core biopsy samples compared to corresponding resection specimen in breast cancer: a multi-operator and multi-institutional study. *Mod Pathol* 35:1362–1369. <https://doi.org/10.1038/s41379-022-01104-9>
- Wang P, Tang Z, Xiao Z et al (2021) Dual-energy CT in predicting Ki-67 expression in laryngeal squamous cell carcinoma. *Eur J Radiol* 140:109774. <https://doi.org/10.1016/j.ejrad.2021.109774>
- Wang X, Liu D, Zeng X et al (2021) Dual-energy CT quantitative parameters for evaluating Immunohistochemical biomarkers of invasive breast cancer. *Cancer Imaging* 21:4. <https://doi.org/10.1186/s40644-020-00370-7>
- Mao LT, Chen WC, Lu JY et al (2023) Quantitative parameters in novel spectral computed tomography: assessment of Ki-67 expression in patients with gastric adenocarcinoma. *World J Gastroenterol* 29:1602–1613. <https://doi.org/10.3748/wjg.v29.i10.1602>
- Noid G, Godfrey G, Hall W et al (2023) Predicting treatment response from extracellular volume fraction for chemoradiation therapy of pancreatic cancer. *Int J Radiat Oncol Biol Phys* 115:803–808. <https://doi.org/10.1016/j.ijrobp.2022.09.084>
- Fujita N, Ushijima Y, Itoyama M et al (2023) Extracellular volume fraction determined by dual-layer spectral detector CT: Possible role in predicting the efficacy of preoperative neoadjuvant chemotherapy in pancreatic ductal adenocarcinoma. *Eur J Radiol* 162:110756. <https://doi.org/10.1016/j.ejrad.2023.110756>
- Nakahodo J, Kikuyama M, Fukumura Y et al (2022) Focal pancreatic parenchyma atrophy is a harbinger of pancreatic cancer and a clue to the intraductal spreading subtype. *Pancreatol* 22:1148–1158. <https://doi.org/10.1016/j.pan.2022.10.003>
- Vasen HFA, Boekstijn B, Ibrahim IS et al (2019) Dilatation of the main pancreatic duct as first manifestation of small pancreatic ductal adenocarcinomas detected in a hereditary pancreatic cancer surveillance program. *HPB (Oxford)* 21:1371–1375. <https://doi.org/10.1016/j.hpb.2019.02.013>
- Zaky AM, Wolfgang CL, Weiss MJ, Javed AA, Fishman EK, Zaheer A (2017) Tumor-vessel relationships in pancreatic ductal adenocarcinoma at multidetector CT: different classification systems and their influence on treatment planning. *Radiographics* 37:93–112. <https://doi.org/10.1148/rg.2017160054>
- Guo X, Gao S, Yu J, Zhou Y, Gao C, Hao J (2021) The imaging features of extrapancreatic perineural invasion (EPNI) in pancreatic Cancer: a comparative retrospective study. *Pancreatol* 21:1516–1523. <https://doi.org/10.1016/j.pan.2021.08.010>

21. Myoteri D, Dellaportas D, Lykoudis PM, Apostolopoulos A, Marinis A, Zizi-Sermpetzoglou A (2017) Prognostic evaluation of vimentin expression in correlation with Ki67 and CD44 in surgically resected pancreatic ductal adenocarcinoma. *Gastroenterol Res Pract* 2017:9207616. <https://doi.org/10.1155/2017/9207616>
22. Nurmi A, Mustonen H, Parviainen H, Peltola K, Haglund C, Seppänen H (2018) Neoadjuvant therapy offers longer survival than upfront surgery for poorly differentiated and higher stage pancreatic cancer. *Acta Oncol* 57:799–806. <https://doi.org/10.1080/0284186X.2017.1415458>
23. Jamieson NB, Carter CR, McKay CJ, Oien KA (2011) Tissue biomarkers for prognosis in pancreatic ductal adenocarcinoma: a systematic review and meta-analysis. *Clin Cancer Res* 17:3316–3331. <https://doi.org/10.1158/1078-0432.CCR-10-3284>
24. Tseng DS, van Santvoort HC, Feghali S et al (2014) Diagnostic accuracy of CT in assessing extra-regional lymphadenopathy in pancreatic and peri-ampullary cancer: a systematic review and meta-analysis. *Surg Oncol* 23:229–235. <https://doi.org/10.1016/j.suronc.2014.10.005>
25. Bi L, Liu Y, Xu J et al (2021) A CT-based radiomics nomogram for preoperative prediction of lymph node metastasis in periampullary carcinomas. *Front Oncol* 29:632176. <https://doi.org/10.3389/fonc.2021.632176>
26. Zopfs D, Reimer RP, Sonnabend K et al (2021) Intraindividual consistency of iodine concentration in dual-energy computed tomography of the chest and abdomen. *Invest Radiol* 56:181–187. <https://doi.org/10.1097/RLI.0000000000000724>
27. Vohra R, Wang YN, Son H et al (2022) Non-invasive monitoring of increased fibrotic tissue and hyaluronan deposition in the tumor micro-environment in the advanced stages of pancreatic ductal adenocarcinoma. *Cancers (Basel)* 14:999. <https://doi.org/10.3390/cancers14040999>

Publisher's Note

Springer Nature remains neutral with regard to jurisdictional claims in published maps and institutional affiliations.